Accepted Manuscript

Improved conversion efficiency and beam quality of miniaturized mid-infrared idler-resonant MgO:PPLN optical parametric oscillator pumped by all-fiber laser

Yang He, Fei Chen, Deyang Yu, Kuo Zhang, Qikun Pan, Junjie Sun

PII: S1350-4495(18)30586-3
DOI: https://doi.org/10.1016/j.infrared.2018.10.002
Reference: INFPHY 2716

To appear in: *Infrared Physics & Technology*

Received Date: 9 August 2018
Revised Date: 30 September 2018
Accepted Date: 1 October 2018

Please cite this article as: Y. He, F. Chen, D. Yu, K. Zhang, Q. Pan, J. Sun, Improved conversion efficiency and beam quality of miniaturized mid-infrared idler-resonant MgO:PPLN optical parametric oscillator pumped by all-fiber laser, *Infrared Physics & Technology* (2018), doi: https://doi.org/10.1016/j.infrared.2018.10.002

Improved conversion efficiency and beam quality of miniaturized mid-infrared idler-resonant MgO:PPLN optical parametric oscillator pumped by all-fiber laser

Yang He [a,b], Fei Chen [a,*], Deyang Yu [a,b], Kuo Zhang [a], Qikun Pan [a], Junjie Sun [a]

[a] *State Key Laboratory of Laser Interaction with Matter, Innovation Laboratory of Electro-Optical Countermeasures Technology, Changchun Institute of Optics, Fine Mechanics and Physics, Chinese Academy of Sciences, 3888 Dongnanhu Road, Changchun Jilin 130033, China*

[b] *University of Chinese Academy of Sciences, Beijing 100049, China*

* *feichenny@126.com*

Abstract

We present a miniaturized idler-resonant all-fiber-laser-pumped optical parametric oscillator (OPO) based on MgO:PPLN. The conversion-efficiency and beam-quality performances of the idler- and signal-resonant OPOs with flat-flat cavity are first compared. The idler-resonant OPO MIR beam quality is better than that of the signal-resonant one, but the idler conversion efficiency is lower. Next, we examine the influence of the output-coupler curvature radius, pump-beam-waist radius, and cavity length on the MIR conversion efficiency and beam quality of the idler-resonant OPO. Post optimization of these factors, we report a maximum MIR power of 5.84 W at 3.76 μm, conversion efficiency >14.0%, and M^2 factors of 1.57 and 1.49 along the horizontal and vertical directions, respectively.

Keywords: Optical parametric oscillator; MgO:PPLN; Mid-infrared; Idler-resonant; Miniaturized; All-fiber-laser pumped

1. Introduction

The mid-infrared (MIR) spectral region of the electromagnetic spectrum corresponds to the atmospheric transmission window and several important molecular absorption lines. Consequently, MIR laser sources have become desirable for applications, such as, atmosphere monitoring, laser spectroscopy, photoelectric detection, and remote sensing surveys [1–6]. In these applications, optical parametric oscillators (OPOs) are a proven approach to realize MIR lasers from the continuous wave (CW) to ultrafast regimes [7–14]. In particular, high-efficiency miniaturized MIR lasers with high beam quality are of paramount importance. In this regard, fiber-laser-pumped MgO-doped periodically poled lithium niobate (MgO:PPLN) OPOs have the ability to convert near-infrared radiation into MIR with high efficiency and high beam quality. Further, with their benefits of small size, light weight, and excellent heat dissipation, fiber-laser-pumped MgO:PPLN OPOs have attracted considerable research interest in recent years. In general, fiber-laser-pumped MgO:PPLN OPOs adopt the signal-resonant configuration, wherein only the signal wave oscillates in the cavity. In this regard, Lin et al. demonstrated a signal-resonant MgO:PPLN-based OPO pumped by a nanosecond-pulse linearly polarized fiber laser, which generated 5.5 W at 3.82 μm with an optical-to-optical conversion efficiency of ~9.5% [15]. Further, Liu et al. reported a tunable signal-resonant MgO:PPLN OPO pumped by a Yb fiber laser, and they obtained MIR output powers of 1.03 W and 0.67 W at 3.7 μm and 3.9 μm with conversion efficiencies of 14.3% and 9.3%, respectively [16]. Shang et al. demonstrated a CW signal-resonant OPO using MgO:PPLN pumped by an amplified random fiber laser. An idler output power of 2.46 W at 3752 nm was achieved, and the conversion efficiency was 9.6% at room temperature. Further, the beam quality M^2 factors were ~1.24 and ~1.16 along the horizontal and vertical directions, respectively [17]. Meanwhile, Shukla et al. presented a signal-resonant MgO:PPLN-based OPO pumped by a Yb fiber laser, with which a maximum power of 2 W was achieved at 3895 nm with optical-to-optical conversion efficiency of ~12.5%. Further, the M^2 value for the MIR beam was measured to be less than 1.34 [18].

However, in all these approaches, when the MIR wavelength exceeds 3.5 μm, the absorption of the MgO:PPLN crystal is high. With high pump power, the MgO:PPLN crystal generates strong thermal lensing effects [15], which degrades the beam quality of the non-resonant idler. To overcome this problem, the idler-resonant configuration can be used instead of the signal-resonant one. With its resonance in the cavity, the idler can be constrained by the cavity mirrors [19], and the thermal lensing effects on the idler can be reduced, thereby yielding improved MIR beam quality. Via optimizing the parameters of the idler-resonant OPO, the MIR conversion efficiency can also be enhanced. In this regard, it was demonstrated in a femtosecond-fiber-laser-pumped idler-resonant OPO operating in the range of 2.2-2.6 μm that the idler beam quality (M^2 ~ 1.05) was near-diffraction-limited. The idler average power was 600 mW and the conversion efficiency was ~13.3% [14]. Along these lines, Parsa et al. reported on an idler-resonant MgO:PPLN OPO pumped by a picosecond Yb-fiber amplifier; the M_x^2 and M_y^2 values of the idler at 3.34 μm were ~1.1 and ~1.02, respectively, and the average idler power was 1 W with a conversion efficiency of ~9.1% [20].

Against this backdrop, in this paper, we report on a miniaturized idler-resonant MgO:PPLN-based OPO operating at ~3.8 μm. The pump source is a high-power linearly polarized all-fiber laser. The performance of the idler-resonant OPO is firstly compared with the signal-resonant one. Subsequent experiments are carried out to explore how the MIR conversion efficiency and beam quality of the idler-resonant OPO are influenced by the curvature radius of the output coupler R, radius of the pump beam waist ω, and length of the cavity L. Via optimization of R, ω, and L, both the idler conversion efficiency and beam quality are improved. Our miniaturized idler-resonant OPO achieves a maximum MIR power of 5.84 W at 3.76 μm with a conversion efficiency of more than 14.0%. To the best of our knowledge, this is the highest MIR power and conversion efficiency above 3.7 μm reported thus far with the use of the fiber-laser-pumped idler-resonant MgO:PPLN-based OPO configuration. The corresponding M^2 factors of the idler along the horizontal and vertical directions are 1.57 and 1.49, respectively.

2. Description of miniaturized OPO

The schematic of the miniaturized MgO:PPLN OPO is shown in Fig. 1. It consists of a linearly polarized all-fiber laser module, beam control module, and OPO module. The linearly polarized all-fiber laser module generates a pump laser based on the master oscillator power amplifier (MOPA) structure with the master-oscillation and power-amplifier stages. The master-oscillation stage comprises a linearly polarized distributed feedback (DFB) laser utilized to produce the seed light. The power amplifier stage comprises three-stage linearly polarized

Yb-doped fiber amplifiers (YDFAs) pumped by 976-nm laser diodes (LDs). The polarization-maintaining (PM) Yb-doped fiber (YDF) is coiled to improve the beam quality of the pump laser and reduce the module size. The pump power can reach more than 40 W. The pump laser spectrum is shown in Fig. 2. The wavelength is 1063.6 nm and the line-width is ~3 nm. The full-width at half-maximum (FWHM) pulse duration is ~30 ns at a repetition rate of ~55 kHz. The pump laser is horizontally polarized and collimated to a beam radius of ~1 mm. With the maximum output power, the M^2 factors of the pump laser along the horizontal and vertical directions are 1.29 and 1.24, respectively.

The beam control module mainly consists of a Faraday isolator and a lens group. The Faraday isolator can protect the linearly polarized all-fiber laser module from any unwanted reflections. Two half-wave plates are pasted on both ends of the isolator, and they can rotate the polarization of the pump laser to the vertical direction to align along the principal axis of the MgO:PPLN crystal for maximum OPO conversion efficiency. Subsequently, the beam radius of the pump laser is reduced in size by the lens group. By choosing different combinations of focal-length lenses, we can set the radius of the pump beam waist ω to required values.

Next, the pump laser is coupled into the MgO:PPLN crystal of the OPO module. The dimensions of the MgO:PPLN crystal are 50 mm × 3 mm × 2 mm, and the grating period is 29.5 μm. Both ends of the MgO:PPLN crystal are antireflection-coated for wavelengths of 1.06 μm, 1.48 μm, and 3.8 μm. The crystal is placed in a temperature control oven, which has a precision of ±0.1 °C. The oven temperature is set to 65 °C, which corresponds to signal and idler wavelengths of ~1.48 μm and ~3.8 μm, respectively. The resonant cavity consists of a flat input mirror and an output coupler. The input mirror is antireflection-coated at 1.06 μm and high-reflection-coated at 1.48 μm and 3.8 μm. The output coupler is high-reflection-coated at 1.06 μm. The location of MgO:PPLN crystal is always at the center of the cavity. The OPO process occurs due to the feedback effect of the resonant cavity, which affords the NIR signal laser and the MIR idler laser output. A dichroic mirror is used to filter out the signal and achieve the MIR laser output.

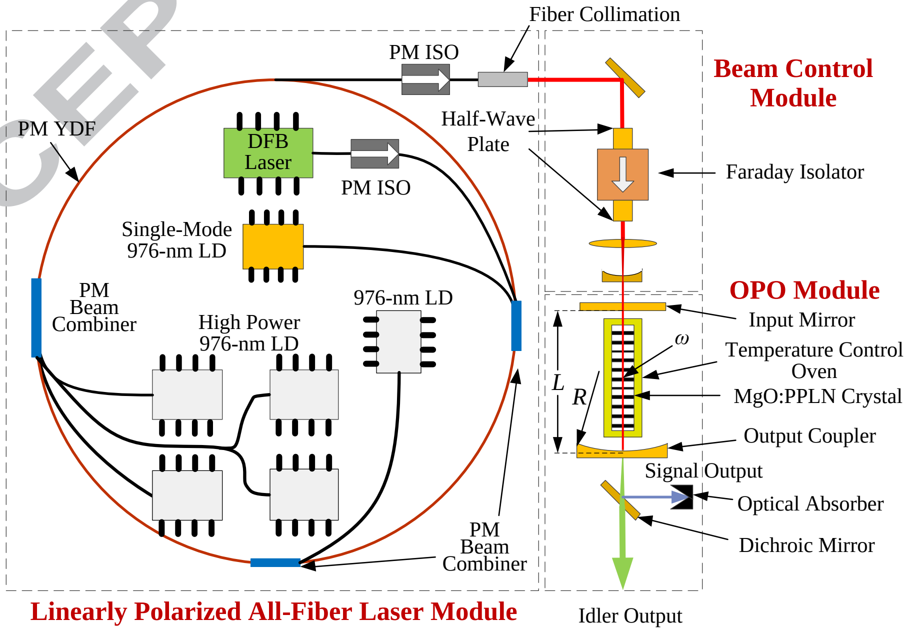

Fig.1. Schematic of linearly polarized all-fiber-laser-pumped miniaturized optical parametric oscillator (OPO) based on MgO:PPLN.

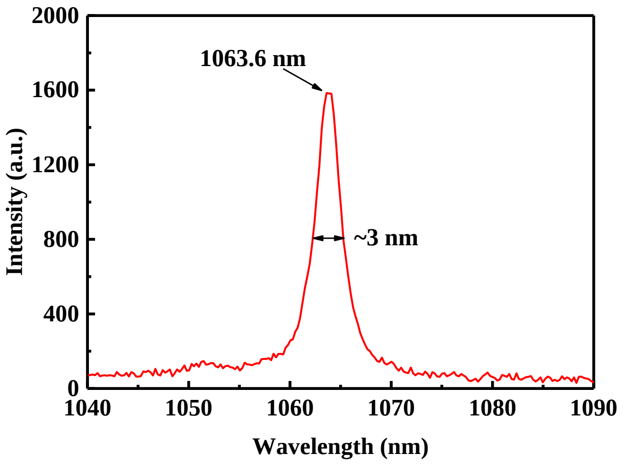

Fig.2. Spectrum of the linearly polarized all-fiber laser module

During OPO operation, the linearly polarized all-fiber laser module generates a large amount of waste heat that needs to be dissipated without delay; otherwise, this heat can cause wavelength shift, decrease in output power, and even damage the laser. Therefore, in our study, we designed a thermal control system [21] to remove the waste heat. For miniaturization, the thermal control system of the OPO adopts the thermoelectric cooling configuration, which has the advantages of compact size, light weight, high reliability, and the absence of liquid over conventional water cooling. It is composed of thermoelectric coolers (TECs), an aluminum cabinet with cooling fins, axial fans, and heat pipes. As shown in Fig. 3, the heat sink of the linearly polarized all-fiber laser module is affixed to the cold side of the TECs, while the hot side of the TECs is tightly affixed to the bottom of the aluminum cabinet. During laser operation, the waste heat generated from the linearly polarized all-fiber laser module is absorbed by the TECs and transferred to the bottom of the aluminum cabinet with cooling fins. The axial fans are fixed on one side of the cooling fins to increase the heat convection coefficient through forced convection cooling. There are also two heat pipes fixed at the bottom of the laser cabinet to improve the heat transfer performance of the system. With the thermal control system, the size of the whole miniaturized OPO is only 330 mm × 330 mm × 165 mm. The corresponding weight is <10 kg.

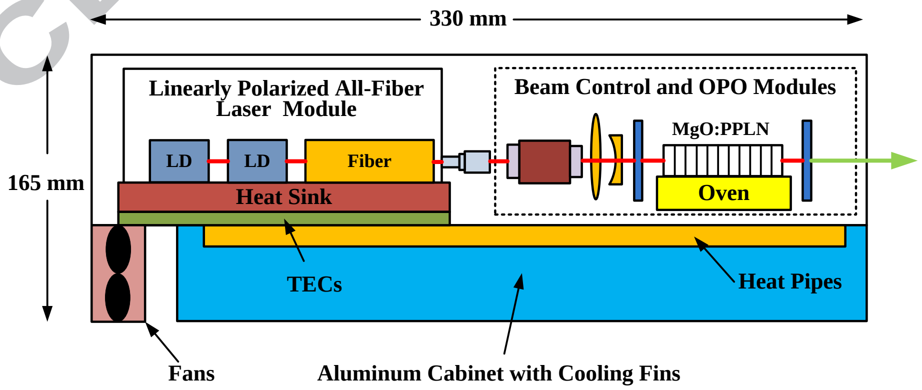

Fig. 3. Schematic of thermal control system for optical parametric oscillator (OPO).

3. Results and discussion

3.1 Comparison of signal-resonance and idler-resonance

In our study, we firstly investigated the characteristics of the signal-resonant and idler-resonant OPOs. For signal-resonance, the output coupler was antireflection-coated at 3.8 μm and for ~70% reflection at 1.48 μm. For idler-resonance, the output coupler was antireflection-coated at 1.48 μm and for ~70% reflection at 3.8 μm. Both output couplers were flat, and the length of the cavity L was set to 75 mm. We ensured that the pump beam waist lay at the center of the MgO:PPLN crystal, and the beam radius ω was 280 μm.

The idler output power and conversion efficiency of the signal-resonant OPO and idler-resonant OPO configurations are shown in Fig. 4. It can be observed that the output power and conversion efficiency with idler-resonance are less than the corresponding ones with signal-resonance. Further, when the pump power is 26.8 W, the MIR powers of the idler-resonant OPO and the signal-resonant OPO are 2.36 W and 4.03 W with conversion efficiencies of 8.8% and 14.9%, respectively. The above results show that when the idler resonates in the cavity, the absorption loss caused by MgO:PPLN crystal and the diffraction loss make the idler output power lower, as well as the conversion efficiency.

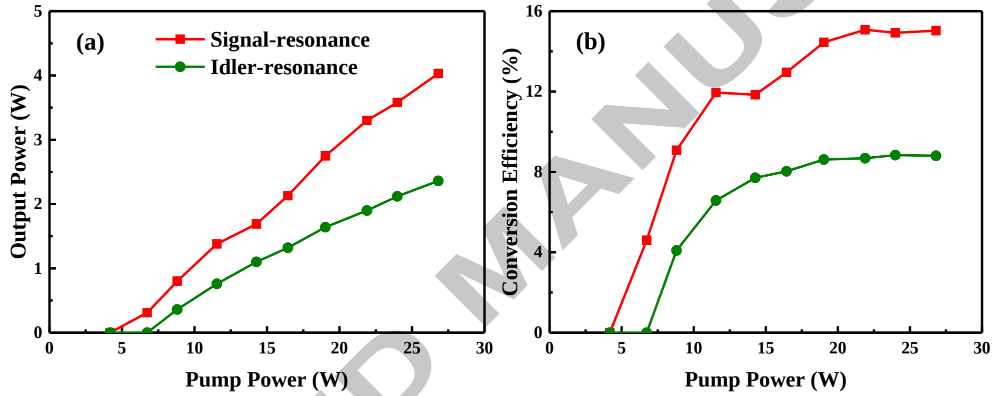

Fig. 4. Idler (a) output power and (b) conversion efficiency as functions of pump power for signal-resonance and idler-resonance.

The beam quality of the idler laser was measured by means of the knife-edge method. For an MIR output power of 2 W, the idler M^2 factors of the signal-resonant OPO were 2.77 along the horizontal direction and 2.54 along the vertical direction. Further, the M^2 factors of the idler-resonant OPO along the horizontal and vertical directions were 1.22 and 1.18, respectively. This experimental result demonstrates that the idler-resonant OPO exhibits better idler beam quality when using the flat–flat cavity. The near-field beam profiles of both OPOs are shown in Fig. 5.

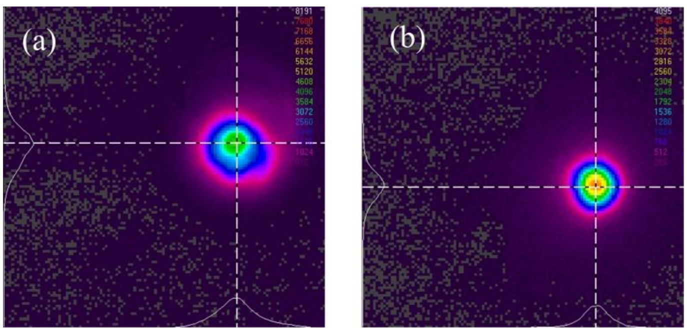

Fig. 5. Near-field idler beam profiles of (a) signal-resonant optical parametric oscillator (OPO) and (b) idler-resonant OPO for output power of 2 W.

3.2 Improvement in MIR conversion efficiency with idler-resonance

3.2.1 Influence of curvature radius of output coupler *R*

Although the MIR beam quality of the idler-resonant OPO with the flat–flat cavity is better than that of the signal-resonant one, the MIR power and conversion efficiency are relatively lower. To improve the MIR conversion efficiency, we changed the cavity to a plane–concave one, and we varied the curvature radius of output coupler *R* as 100 mm, 200 mm, 300 mm, and 500 mm. The other experimental conditions were the same as in the previous case.

The output power and conversion efficiency of the idler-resonant OPO as functions of the pump power for different output couplers are shown in Fig. 6. It can be observed that the plane–concave cavity contributes to improve the idler output power and conversion efficiency. Smaller *R* values correspond to larger MIR powers and conversion efficiencies. Because when the pump laser is reflected back to the crystal by the output coupler, the radius of pump laser decreases with *R* reducing. The conversion efficiency becomes larger due to the higher pump power density. However, when *R* = 100 mm, the focal point of the output coupler lies within the MgO:PPLN crystal, which can damage the crystal when the pump power is more than 23 W. Therefore, *R* cannot be so small that the laser focus lies within the crystal. The output coupler with a curvature radius of 200 mm was found suitable in this experiment. Further, with the maximum pump power, the idler power and conversion efficiency reached 3.53 W and 13.2%, respectively.

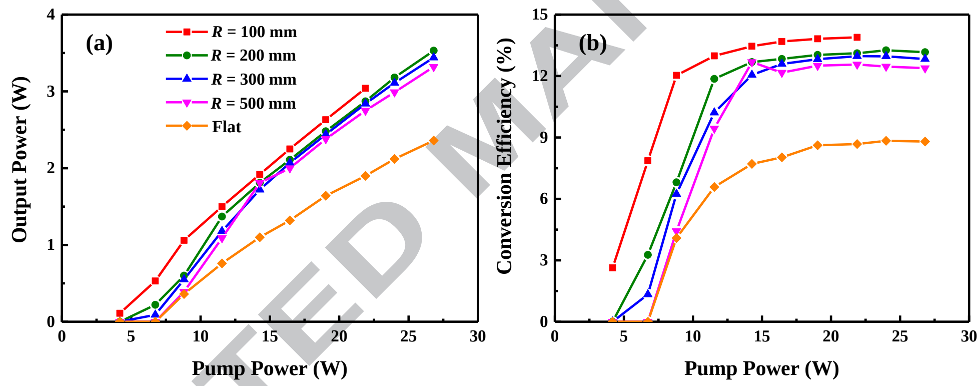

Fig. 6. Idler (a) output power and (b) conversion efficiency versus pump power for different curvature radii of output coupler *R*.

3.2.2 Influence of radius of pump laser waist ω

The dependence of the idler conversion efficiency on the radius of the pump laser waist ω was also investigated. Upon fixing the curvature radius of the output coupler as 200 mm, we varied ω as 200 μm, 220 μm, 280 μm, and 325 μm, with the other experimental conditions of the idler-resonant OPO remaining the same as the previous cases. The results are summarized in Fig. 7. We observe that the idler power and conversion efficiency improve with decrease in ω. The maximum MIR power of 3.72 W with conversion efficiency of 13.9% is obtained for ω = 200 μm. The above results can be explained as follows: when the beam waist is small, a higher pump power density contributes to increasing OPO conversion efficiency. However, ω cannot be too small; otherwise, the MgO:PPLN crystal will suffer damage due to the increased pump power density at the waist.

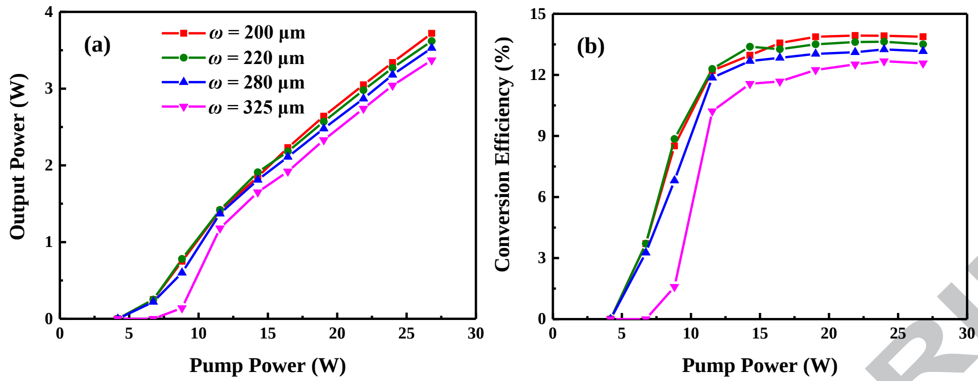

Fig. 7. Idler (a) output power and (b) conversion efficiency versus pump power for different radii of pump laser waist ω.

3.2.3 Influence of length of cavity *L*

The length of the cavity *L* also influences the conversion efficiency of the idler-resonant OPO. To investigate this aspect, we set *R* and ω to be 200 mm and 220 μm, respectively. Next, *L* was varied as 65 mm, 75 mm, 85 mm, and 100 mm, with other experimental conditions remaining unchanged. Figure 8 shows the MIR power and conversion efficiency of the idler-resonant OPO as functions of the pump power for different cavity lengths. Obviously, as *L* reduces, the idler power and conversion efficiency correspondingly increase. When L = 65 mm, the maximum MIR power can reach 3.82 W along with a conversion efficiency of 14.2%.

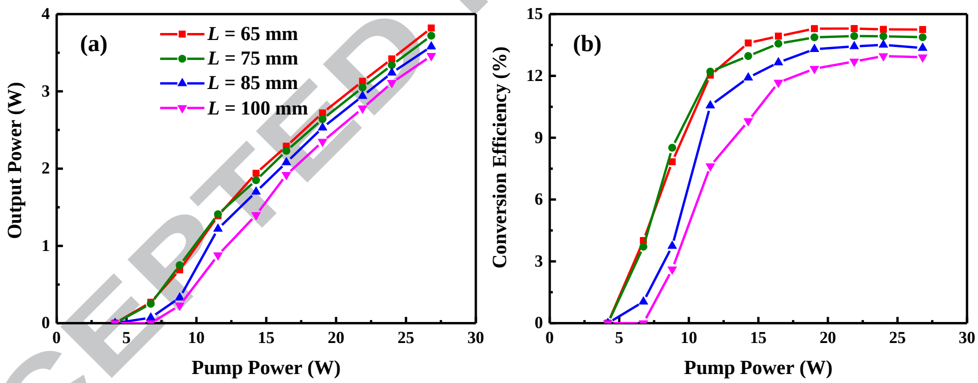

Fig. 8. Idler (a) output power and (b) conversion efficiency versus pump power for different cavity lengths *L*.

3.3 MIR beam quality with idler-resonance

The idler beam quality was next measured by use of the knife-edge method along the horizontal and vertical directions. Figure 9 depicts the idler beam quality when the MIR output power is 2 W. From Fig. 9(a), it can be observed that smaller *R* values can degrade the MIR beam quality. By calculating, when *R* is 200 mm, 300 mm, and 500 mm, the idler fundamental cavity mode radii at the center of MgO:PPLN crystal are ~492 μm, ~606 μm, and ~800 μm, respectively. As *R* reduces, the idler fundamental cavity mode radius decreases, and the radii of higher-order transverse modes also decrease. Therefore, the smaller *R* makes the diffraction loss of the higher-order transverse modes small, which degrades the MIR beam quality. Further, smaller ω values yield improved M^2 factors, as shown in Fig. 9(b). The smaller spatial size of the pump beam restricts the idler laser in terms of higher-order transverse modes generation, which improves the idler beam quality. As regards beam quality as a function of the cavity length *L*, as shown in Fig. 9(c), the idler beam quality improves for larger L values, which indicates that larger L values aid in suppressing the generation of higher-order transverse modes.

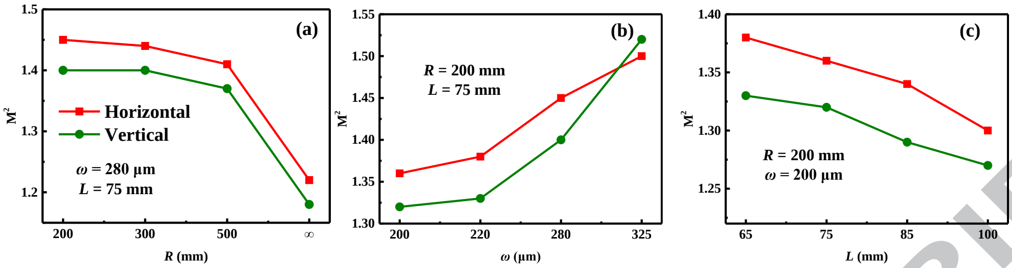

Fig. 9. Idler M^2 factors along horizontal and vertical directions as functions of (a) coupling radius R, (b) pump beam waist ω, and (c) cavity length L for output power of 2 W.

3.4 Optimization of miniaturized idler-resonant OPO

The abovementioned results indicate that the idler power and conversion efficiency are optimal when R, ω, and L are 200 mm, 200 μm, and 65 mm, respectively. Further, for an output power of 2 W, the MIR M^2 factors are less than 1.40. Figure 10(a) depicts the MIR power and conversion efficiency as functions of the pump power (increased up to 41.6 W) for the abovementioned settings; the maximum MIR power can reach 5.84 W and the corresponding conversion efficiency is >14.0%. And the maximum signal power is 18.24 W. The corresponding MIR spectrum and near-field beam profile are shown in Fig. 10(b). At full output power, the idler wavelength is 3.76 μm and the M^2 factors of the idler along the horizontal and vertical directions are 1.57 and 1.49, respectively. With the use of a beam shaping system, the miniaturized idler-resonant OPO can yield an output MIR power >5 W, as shown in Fig. 11. The stability of MIR power is better than ±1% over 2 hours. In room temperature, the maximum electric power consumption of the whole OPO system is ~215 W and the MIR wall-plug efficiency is ~2.7%.

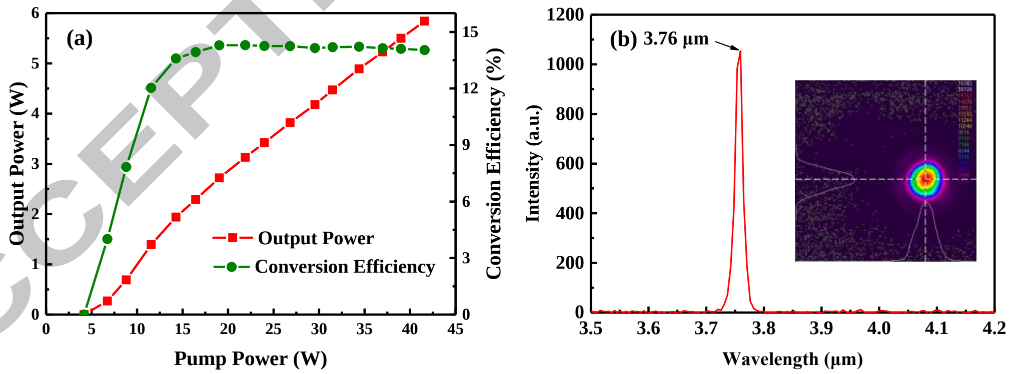

Fig. 10. Mid-infrared (MIR) (a) output power, conversion efficiency, and (b) spectrum and beam profile of miniaturized idler-resonant optical parametric oscillator (OPO) when R, ω, and L are 200 mm, 200 μm, and 65 mm, respectively.

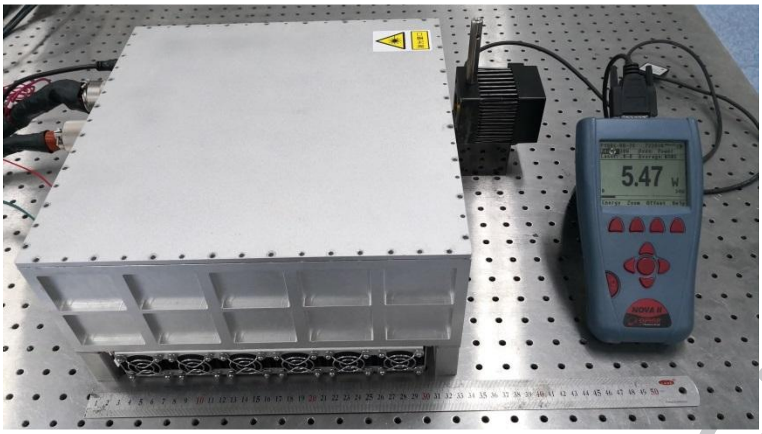

Fig. 11. Photograph showing measured mid-infrared (MIR) output power of our miniaturized idler-resonant optical parametric oscillator (OPO).

4 Conclusion

In our study, we proposed and designed a miniaturized linearly polarized all-fiber-laser-pumped MIR idler-resonant OPO based on MgO:PPLN. Firstly, we compared the idler conversion efficiency and beam quality of the idler-resonant and the signal-resonant OPOs. Although the MIR beam quality of the idler-resonant OPO was higher, the MIR conversion efficiency with the flat–flat cavity was found to be unsatisfactorily low. Subsequently, we experimentally investigated the idler conversion efficiency and beam quality of the idler-resonant OPO as functions of curvature radius of the output coupler R, radius of the pump beam waist ω, and length of cavity L. Our results indicated that the idler conversion efficiency increases with decrease in R, ω, and L. Further, larger R, smaller ω, and larger L values contribute to enhancing the idler beam quality. To achieve a high MIR conversion efficiency and beam quality, we set R, ω, and L as 200 mm, 200 μm, and 65 mm, respectively. For this setting, with increase in the pump power, the miniaturized idler-resonant OPO afforded a maximum MIR power of 5.84 W at 3.76 μm with a conversion efficiency >14.0%. To the best of our knowledge, this is the highest MIR power and conversion efficiency above 3.7 μm till now by using the fiber laser pumped idler-resonant MgO:PPLN based OPO configuration. The corresponding M^2 factors of the idler along the horizontal and vertical directions were 1.57 and 1.49, respectively. In conclusion, we believe that our experimental results will be useful in designing miniaturized MIR idler-resonant MgO:PPLN-based OPO systems with high conversion efficiency and high beam quality.

Acknowledgements

The authors want to acknowledge the support provided by ‘Open Fund Project of the State Key Laboratory of Laser and Material Interaction’ (Grant No. SKLLIM1713), ‘National Natural Science Foundation of China’ (Grant No. 61705219), ‘Major Science and Technology Biding Project of Jilin Province’ (Grant No. 20160203016GX), ‘Young and Middle-Aged Science and Technology Innovation Leader and Team Project of Jilin Province’ (Grant No. 20170519012JH) and ‘Youth Innovation Promotion Association of CAS’ (Grant No. 2017259).

Reference

[1] G. V. Basum, D. Halmer, P. Hering, M. Mürtz, S. Schiller, F. Müller, A. Popp, and F. Kühnemann, Parts per trillion sensitivity for ethane in air with an optical parametric oscillator cavity leak-out spectrometer, Opt. Lett. 29 (8) (2004) 797-799.

[2] Y. Zhang, F. Wang, Y. Zhao, Y. Wang, T. Cui, R. Kan, L. Wu, T. Zhang, Y. Zhang, Experiment research on ellipsoidal structure methane using the absorption characteristics of 3.31 μm mid-infrared spectroscopy Infrared Phys. Technol. 55 (4) (2012) 353-356.

[3] T. Steinle, V. Kumar, M. Floess, A. Steinmann, M. Marangoni, C. Koch, C. Wege, G. Gerullo, and H. Giessen, Synchronization-free all-solid-state laser system for stimulated Raman scattering microscopy, Light Sci. Appl. 5 (10) (2016) e16149.

[4] M. Yan, P. L. Luo, K. Iwakuni, G. Millot, T. W. Hansch, and N. Picque, Mid-infrared dual-comb spectroscopy with electro-optic modulators, Light Sci. Appl. 6 (10) (2017) e17076.

[5] Sheng S. Li, Seung-Hwan Kim, Jun-Hee Moon, Jung Hee Lee, A two-stack, multi-color quantum well infrared photodetector for mid- and long-wavelength infrared detection, Infrared Phys. Technol. 44 (4) (2003) 235-241.

[6] P. Weibring, H. Edner, and S. Svanberg, Versatile mobile lidar system for environmental monitoring, Appl. Opt. 42 (18) (2003) 3583-3594.

[7] W. R. Bosenberg, A. Drobshoff, and J. I. Alexander, 93% pump deletion, 3.5-W continuous-wave, singly resonant optical parametric oscillator, Opt. Lett. 21 (17) (1996) 1336-1338.

[8] S. C. Kumar, R. Das, G. K. Samanta, and M. Ebrahim-Zadeh, Optimally-output-coupled, 17.5 W, fiber-laser-pumped continuous-wave optical parametric oscillator, Appl. Phys. B 102 (1) (2011) 31-35.

[9] Y. Zhang, Z. Wang, Q. Zhou, J. Zhang, H. Zhu, C. Xu, and Y. Duan, Efficient intra-cavity continuous-wave periodically poled lithium niobate-doped MgO optical parametric oscillator with compact V-type cavity, Jpn. J. Appl. Phys. 57 (10) (2018) 100311.

[10] Y. Zhang, Y. Duan , Z. Wang, D. Zhang, J. Zhang, Y. Zhang, and H. Zhu, Continuous-wave widely tunable MgO:PPLN optical parametric oscillator with compact linear cavity, IEEE Photon. Technol. Lett. 30 (20) (2018) 1756-1759.

[11] Y. Peng, X. Wei, W. Wang, and D. Li, High-power 3.8 μm tunable optical parametric oscillator based on PPMgO:CLN, Opt. Common. 283 (20) (2010) 4032-4035.

[12] Kokabee, A. Esteban-Martin, and M. Ebrahim-Zadeh, Efficient, high-power, ytterbium-fiber-laser-pumped picosecond optical parametric oscillator, Opt. Lett. 35 (19) (2010) 3210-3212.

[13] K. A. Tillman, D. T. Reid, D. Artigas, and T. Y. Jiang, Idler-resonant femtosecond tandem optical parametric oscillator tuning from 2.1 μm to 4.2 μm, J. Opt. Soc. Am. B 21 (8) (2004) 1551-1558.

[14] L. Xu, J. S. Feehan, L. Shen, A. C. Peacock, D. P. Shepherd, D. J. Richardson, and J. H. V. Price, Yb-fiber amplifier pumped idler-resonant PPLN optical parametric oscillator producing 90 femtosecond pulses with high beam quality, Appl. Phys. B 117 (2014) 987-993.

[15] D. Lin, S. Alam, Y. Shen, T. Chen, B. Wu, and D. J. Richardson, Large aperture PPMgLN based high-power optical parametric oscillator at 3.8 μm pumped by a nanosecond linearly polarized fiber MOPA, Opt. Express 20 (14) (2012) 15008-15014.

[16] S. Liu, Z. Wang, B. Zhang, J. He, J. Hou, K. Yang, R. Wang, and X. Liu, Wildly tunable, high-efficiency MgO:PPLN mid-IR optical parametric oscillator pumped by a Yb-fiber laser, Chin. Phys. Lett. 31 (2) (2014) 024204.

[17] Y. Shang, M. Shen, P. Wang, X. Li, and X. Xu, Amplified random fiber laser-pumped mid-infrared optical parametric oscillator, Chin. Opt. Lett. 14 (12) (2016) 121901.

[18] M. K. Shukla and R. Das, High-power single-frequency source in the mid-infrared using a singly resonant optical parametric oscillator pumped by Yb-fiber laser, IEEE J. Sel. Top. Quantum Electron. 24 (5) (2018) 5100206.

[19] F. Bai, Q. Wang, Z. Liu, X. Zhang, W. Lan, X. Tao, and Y. Sun, Idler-resonant optical parametric oscillator

based on $KTiOAsO_4$, Appl. Phys. B 112 (1) (2013) 83-87.

[20] S. Parsa, S. C. Kumar, K. Devi, and M. Ebrahim-Zadeh, High-power, high-beam-quality, idler-resonant mid-infrared picosecond optical parametric oscillator, in High-brightness Sources and Light-driven Interactions Congress 2018 (2018) paper MW2C.6.

[21] D. Yu, Y. He, K. Zhang, Q. Pan, F. Chen, and L. Guo, A tunable mid-infrared solid-state laser with a compact thermal control system, Appl. Sci. 8 (6) (2018) 878.

Conflict of Interest

This manuscript has not been published or presented elsewhere in part or in entirety and is not under consideration by another journal. We have read and understood your journal's policies, and we believe that neither the manuscript nor the study violates any of these. There are no conflicts of interest to declare.

Highlights

- A miniaturized all-fiber-laser pumped mid-infrared (MIR) MgO:PPLN optical parametric oscillator (OPO) is bulit.
- Idler-resonant configuration is used for improving the MIR beam quality.
- Output-coupler curvature radius, pump-beam-waist radius, and cavity length are optimized to improve the MIR conversion efficiency.
- 5.84-W laser at 3.76 μm is obtained with the conversion efficiency >14.0% and M^2 factors of 1.57 and 1.49 along the horizontal and vertical directions, respectively.